GP43C-1261: A lithospheric magnetic field model derived from the *Swarm* satellite magnetic field measurements

Thébault E.[1], P. Vigneron[2], and G. Hulot[2]

[1]LPG Nantes, University of Nantes, France.

[2]Institut de Physique du Globe de Paris, UMR CNRS 7154, 1 rue Jussieu F-75005 Paris, France.

Abstract

The Swarm constellation of satellites was launched in November 2013 and has since then delivered high quality scalar and vector magnetic field measurements. A consortium of several research institutions was selected by the European Space Agency (ESA) to provide a number of scientific products which will be made available to the scientific community. Within this framework, specific tools were tailor-made to better extract the magnetic signal emanating from Earth's the lithospheric. These tools rely on the vector and scalar gradients measured by the lower pair of Swarm satellites and rely on a regional modeling scheme that is more sensitive to small spatial scales and weak signals than the standard spherical harmonic modeling. In this presentation, we report on various activities related to data analysis and processing. We assess the efficiency of this dedicated chain for modeling the lithospheric magnetic field using more than one year of measurements, and finally discuss refinements that are continuously implemented in order to further improve the robustness and the spatial resolution of the lithospheric field

The Algorithm

We apply a procedure developed during the Swarm preparation phase (Thébault et al., 2013). The processing steps to isolate the lithospheric signal are presented in **Figure 1**. The Swarm Level 1b data are first selected and corrected for various sources fields using auxiliary indices and models. We consider the Swarm A and C measurements below 490 km altitude from March 2014 to November 2015 (**Process 1**) . We select night time vector and scalar measurements corresponding to Dst value lower than ±5 nT, Kp index smaller than 2o and |IMFBy| <2nT and IMFBz>0. The selected measurements are then corrected for the main and external magnetic fields which are then complemented by additional built-in processing modules to better correct the data for these source fields (**Process 2 and 3**). After this first set of corrections, the across- and along-track scalar and vector gradients are built and an initial lithospheric field model is computed.

The vector and scalar measurements are corrected for the initial lithospheric field model. Dedicated corrections are then applied along the satellite orbits (**Process 4)** relying mostly on principal component and SH analyses. These additional corrections reduce the offset between adjacent tracks and close encounters.

The modelling approach relies on regional analyses and local functions (Revised Spherical Cap Functions). The inverse problem is solved independently for 600 spherical caps homogeneously distributed in space. Each inverse problem is solved with a robust scheme using Huber weights. All vector and scalar measurements and gradients are considered at latitudes ranging from -52° to 52°. In polar regions, only the vertical component of the field and its horizontal gradient are used in addition to both the scalar and scalar gradient data. Once the regional inversions are completed for all caps, the regional parameters are used to predict the lithospheric vector field values on the nodes of a Gauss-Legendre grid covering the Earth at the *Swarm* data median altitude (about 460 km). These grid values are finally converted into a unique set of spherical harmonics Gauss coefficients without regularization. The dedicated lithospheric field model is the output product of the sequence of these numerical processes.

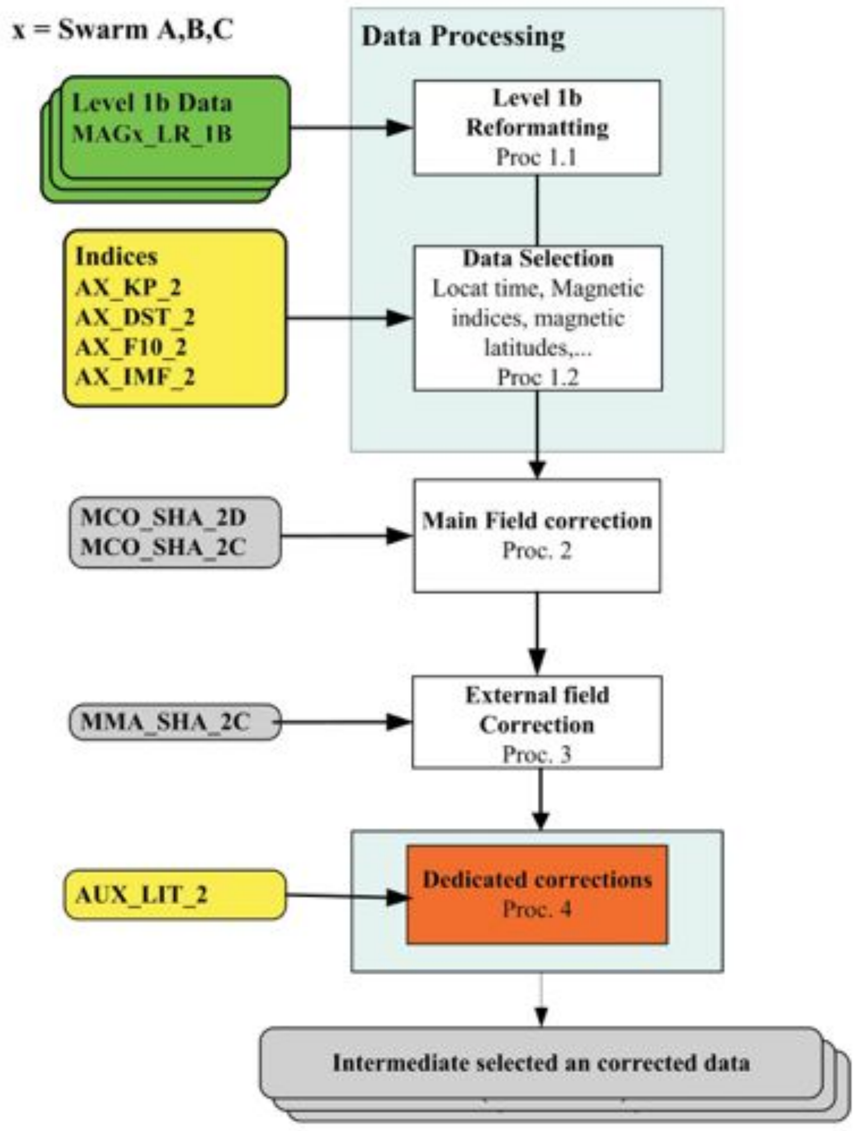

Figure 1: *This flow chart shows the sequence of data selections and corrections that are used to isolate the magnetic field contributions of the Earth's lithosphere.*

Lithospheric field models

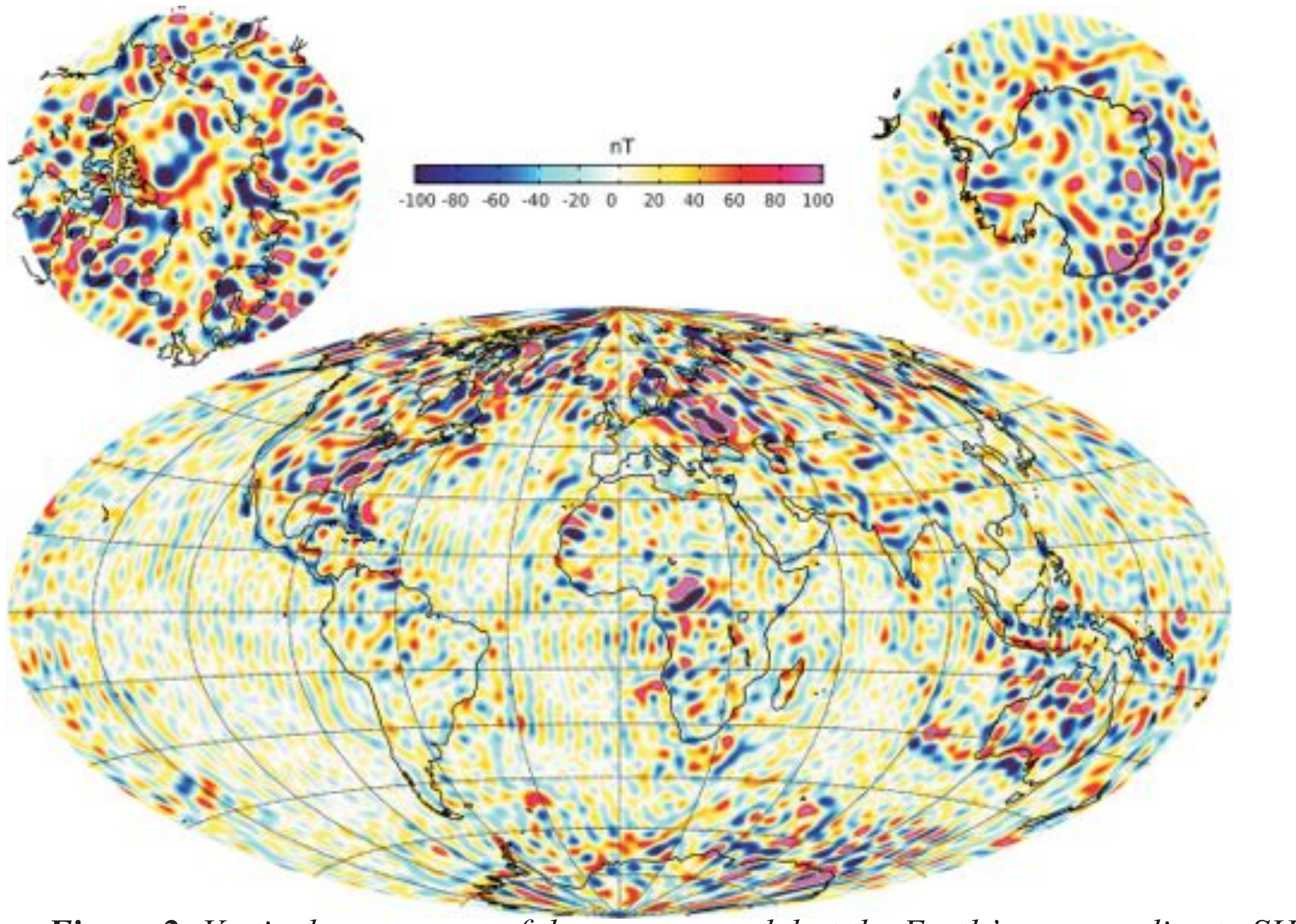

Figure 2: *Vertical component of the present model at the Earth's mean radius to SH degree 80.*

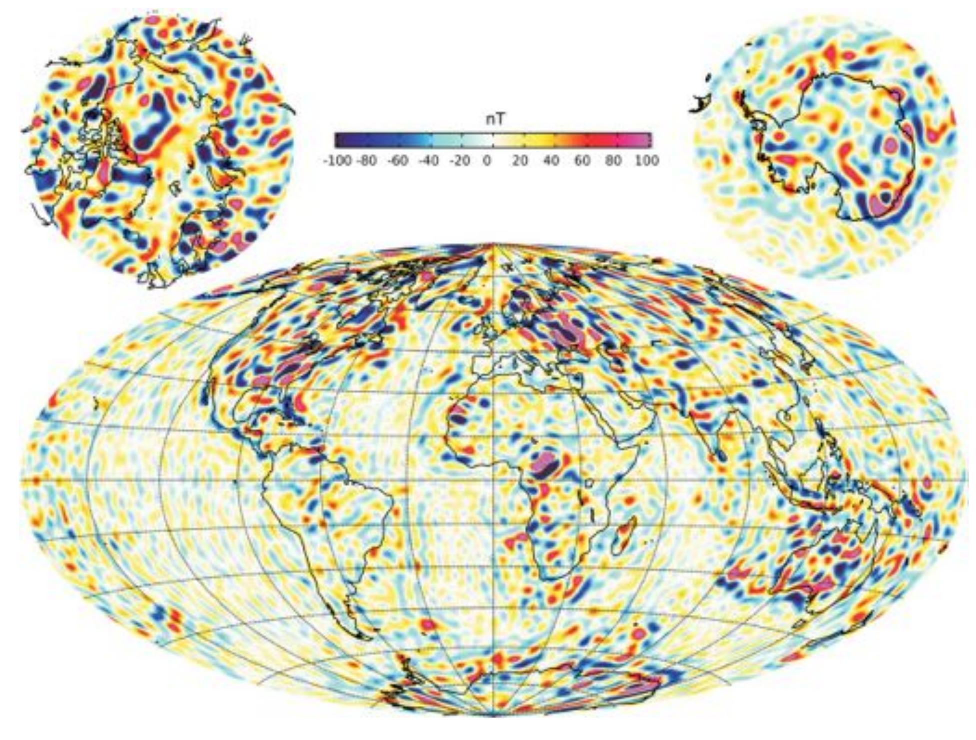

Figure 3: *MF7 lithospheric field to degree 80 from the CHAMP satellite (Maus et al., 2008)*

After two years of measurements, the model suggests that data are (globally) sensitive to crustal field variations up to degree 80 (**Figure 2**). The map compares well with models derived from the CHAMP satellite mission (in operation from epoch 2000 to sept 2009; **Figure 3** for MF7). Differences are strongest in the Northern and Southern Polar regions along the electrojet current structures (**Figure 2**). In these regions, the rapid and significant non-lithospheric contributions lead to arbitrary offsets between adjacent tracks that persist after dedicated correction and filtering. Artefacts are also apparent at mid latitudes along the Swarm satellites orbits in oceanic regions where the lithospheric field is weak. A cleaner separation of the lithospheric signal from ionospheric and magnetospheric noise sources remains however challenging because the root mean square of the crustal field beyond SH degee 80 at 460 km altitude (the median altitude of the Swarm measurements after two years of operation) is about 0.1 nT. This value is comparable to the data calibration uncertainties and the magnetometer instrument noise level. The explicit advantage of using the Swarm gradients is illustrated in **Figure 4**. The misfits are significantly smaller for the gradients than for the vector and scalar measurements, particularly in the polar regions.

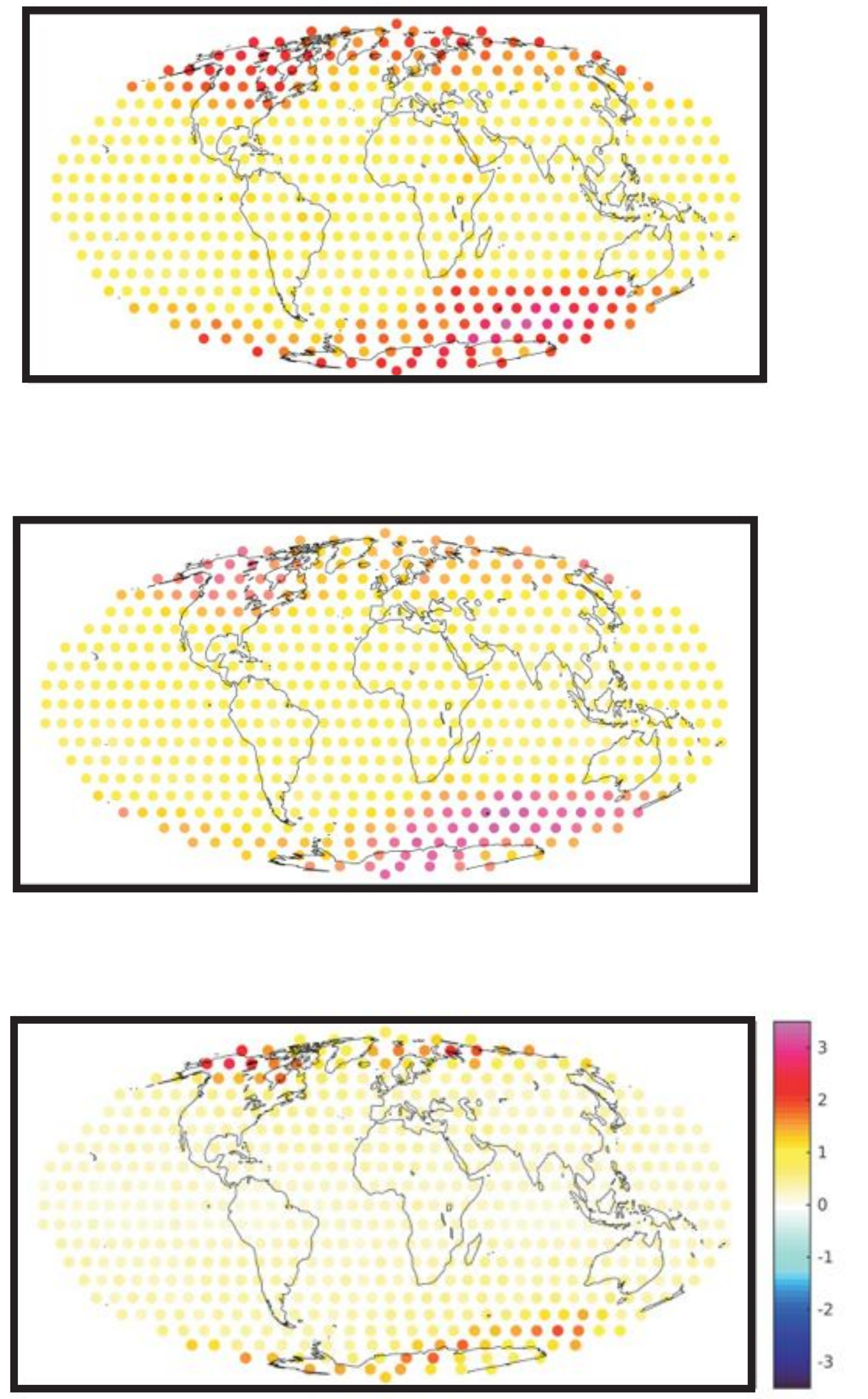

Figure 4 (right): *misfit between the model and the vector components (top), between the model and the scalar components (middle), between the model and the scalar gradients (bottom).*

Maus et al., Resolution of direction of oceanic magnetic lineations by the sixth-generation lithospheric magnetic field model from CHAMP satellite magnetic measurements, Geochem. Geophys. Geosyst., 9, Q07021, doi:10.1029/2008GC001949, 2008.

Thébault E., P. Vigneron, S. Maus, A. Chulliat, O. Sirol, G. Hulot, Swarm SCARF Dedicated Lithospheric Field Inversion chain, Earth Planets and Space, Vol. 65 (No. 11), pp. 1257-1270, 2013 .